

Matching Experimental and Theoretical Jet Definitions for Photoproduction at HERA

J.M. Butterworth^a, L. Feld^b, M. Klasen^c, G. Kramer^c

^a University College London, Physics and Astronomy Dept., London, U.K.

^b Physikalisches Institut der Universität Bonn, Bonn, FRG

^c II. Institut für Theoretische Physik, Universität Hamburg, Hamburg, FRG

Abstract: Predictions from a new next-to-leading order (NLO) calculation for direct and resolved photoproduction of one and two jets are compared to simulated HERA data. We propose a method to match experimental and theoretical jet definitions and observe a reduced dependence on jet definitions and hadronization corrections at larger transverse energies. From the irreducible uncertainty, we estimate the maximum benefit that can be obtained from increased luminosity to constrain the structure of the photon and the proton.

1 Introduction

Hard scattering of real photons off partons can be reliably predicted by perturbative QCD. The first NLO QCD calculation for complete (direct and resolved) photoproduction of one and two jets was completed recently [1]. It is based on the phase space slicing method and uses an invariant mass cut to integrate soft and collinear singularities analytically. The program has successfully been tested with an older existing program in single jet production [2]. In order to be able to compare these theoretical cross sections to experimental data in photoproduction of jets from the ep collider HERA [3, 4], the soft interaction links between initial and final state partons and hadrons have to be under control. Therefore it is only possible to extract new information on the parton densities in the proton and the photon if the jet definitions in the measurement and in the theoretical prediction match. In this paper we propose a method to achieve this for various jet algorithms. The experimental cross sections are simulated for 1994 HERA conditions, where electrons of energy $E_e = 27.5$ GeV collided with protons of energy $E_p = 820$ GeV, using HERWIG 5.8 [5].

2 Jet Definitions

According to the standardization of cone jet algorithms at the Snowmass meeting in 1990 [6], calorimeter cells or partons i are included in a jet, if they have a distance of

$$R_i = \sqrt{(\eta_i - \eta_J)^2 + (\phi_i - \phi_J)^2} \leq R \quad (1)$$

from the jet center and a distance of

$$R_{ij} = \sqrt{(\eta_i - \eta_j)^2 + (\phi_i - \phi_j)^2} \leq \frac{E_{T_i} + E_{T_j}}{\max(E_{T_i}, E_{T_j})} R \quad (2)$$

from each other. Here, $\eta = -\ln[\tan(\theta/2)]$ is the pseudorapidity related to the polar angle θ , and ϕ is the azimuthal angle. If two partons have equal transverse energy they may be separated from each other by as much as $2R$. As parton j does then not lie inside a cone of radius R around parton i and vice versa, one might with some justification also count the two partons separately. If one wants to study only the highest- E_T jet, this “double counting” must be excluded. The definition of an initiating cluster before a cone is introduced (“seed-finding”) is not fixed by the Snowmass convention, and different approaches are possible. The ZEUS collaboration at HERA uses two different cone algorithms: EUCELL takes the calorimeter cells in a window in $\eta - \phi$ space as seeds to find a cone with the highest E_T . The cells in this cone are then removed, and the search is continued. On the other hand, PUCELL was adapted from CDF and starts with single calorimeter cells. It then iterates cones around each of them, until the set of enclosed cells is stable. In this case it may happen that two stable jets overlap. If the overlapping transverse energy amounts to a large fraction of the jets, they are merged, otherwise the overlapping energy is split. In addition, we simulate the same cross sections with the k_T algorithm KTCLUS [7, 8], where particles are combined if their distance

$$d_{ij} = \min(E_{T_i}, E_{T_j})^2 R_{ij}^2 \quad (3)$$

is small. As the same recombination scheme is used, the results are quite similar to the PUCELL results. In the following we choose $R = 1$ throughout. Partonic jets with a large distance of two contributing partons are hard to find because of the missing seed in the jet center. This is especially true for the PUCELL algorithm, which does not perform a preclustering and does indeed find smaller cross sections and different hadronization corrections than the less affected EUCELL algorithm. We propose to model this theoretically by introducing an additional parameter R_{sep} to restrict the distance of two partons from each other [9]. This modifies eq. (2) to

$$R_{ij} \leq \min \left[\frac{E_{T_i} + E_{T_j}}{\max(E_{T_i}, E_{T_j})} R, R_{\text{sep}} \right]. \quad (4)$$

The meaningful range of R_{sep} is between 1 and 2. For two partons of similar or equal transverse energies E_T , R_{sep} is the limiting parameter, whereas it is the parton-jet distance R for two partons with large E_T imbalance. On a NLO three parton final state we find that $R_{\text{sep}} = 1.5\dots 2$ for EUCELL and $R_{\text{sep}} \simeq 1$ for PUCELL and KTCLUS.

3 Results

In figure 1, we show the dijet cross section $d\sigma/d\bar{\eta}$ with $E_T > 6$ GeV and $\Delta\eta = (\eta_1 - \eta_2) \in [-0.5, 0.5]$ for a) direct and b) resolved photoproduction as a function of the average pseudorapidity of the two observed jets $\bar{\eta} = (\eta_1 + \eta_2)/2$. The photon distribution in the electron is taken from the Weizsäcker-Williams approximation with maximum virtuality of $Q_{\text{max}}^2 = 4$ GeV² and longitudinal momentum fraction $y \in [0.2, 0.8]$. The direct and resolved regions are defined by $x_\gamma^{\text{OBS}} > 0.75$ and $x_\gamma^{\text{OBS}} \in [0.3, 0.75]$, where the sum in $x_\gamma^{\text{OBS}} = \frac{\sum_i E_{T_i} e^{-\eta_i}}{2yE_e}$ runs over the two jets

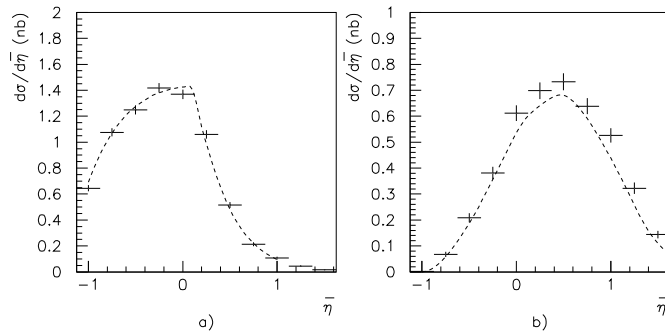


Figure 1: *Demonstration of compatibility of the HERWIG Monte Carlo generator on matrix element level (histograms) and the leading-order (LO) perturbative QCD prediction (curves) for a) direct and b) resolved dijet cross sections $d\sigma/d\bar{\eta}$.*

with largest E_T . In both regions, direct and resolved contributions are added because only their sum is physically meaningful. We demonstrate the compatibility of the two tools used in this study comparing the HERWIG Monte Carlo generator on LO matrix element level and the LO perturbative QCD prediction. We use the CTEQ3L proton and the $\text{GRV}_\gamma(\text{LO})$ photon structure functions. It was not possible to calculate α_s in 1-loop approximation in HERWIG, so we took the (inconsistent) choice of the 2-loop formula for α_s with $\Lambda_{\text{QCD}}^{(4)} = 177$ MeV for this part in the calculation as well. The scales in HERWIG could also not be changed from $\mu^2 = M_\gamma^2 = M_p^2 = 2stu/(s^2 + t^2 + u^2)$, but the effect with respect to using E_T^2 as in the calculation is very small. After these adjustments, HERWIG agrees with the LO QCD prediction.

Figure 2 shows the same cross section for different jet algorithms. We compare our new NLO calculation with jet double counting, without jet double counting, and with $R_{\text{sep}} = 1$ to simulated data from HERWIG with the EUCELL, PUCELL, and KTCLUS algorithms run on the final state particles. In the calculation, we now use a NLO set of input parameters, i.e. CTEQ3M proton, $\text{GRV}_\gamma(\text{HO})$ photon structure functions, and 2-loop α_s with $\Lambda_{\text{QCD}}^{(4)} = 239$ MeV. For the Monte Carlo, we now take HERWIG including parton showers and hadronization. Due to the different parameters used in the NLO calculation and in HERWIG, we do not expect the overall normalization of HERWIG and NLO QCD to agree. However, the relative changes between no R_{sep} (equivalent to $R_{\text{sep}} = 2$) and $R_{\text{sep}} = 1$ on the theoretical side and EUCELL and PUCELL or KTCLUS on the experimental side show the expected similar behaviour, so that the R_{sep} parameter is well suited to match theoretical and experimental jet definitions. Jet double counting does not correspond to an experimental situation and is only shown to illustrate its effect on the theory.

The E_T -dependence of the Snowmass jet definition uncertainties is shown in figure 3 for the a) direct and b) resolved dijet cross sections $d\sigma/dE_T$, where we integrated over the complete $\bar{\eta}$ range and over $\Delta\eta \in [-0.5, 0.5]$. The fractional difference of jet double counting from no double counting amounts to $\sim 20\%$ at 5 GeV and decreases continuously towards larger E_T . Including the parameter $R_{\text{sep}} = 1$ lowers the cross sections by as much as $\sim 40\%$ at 5 GeV, but its influence drops rapidly and gives a constant difference of about 20% (direct) and 10%

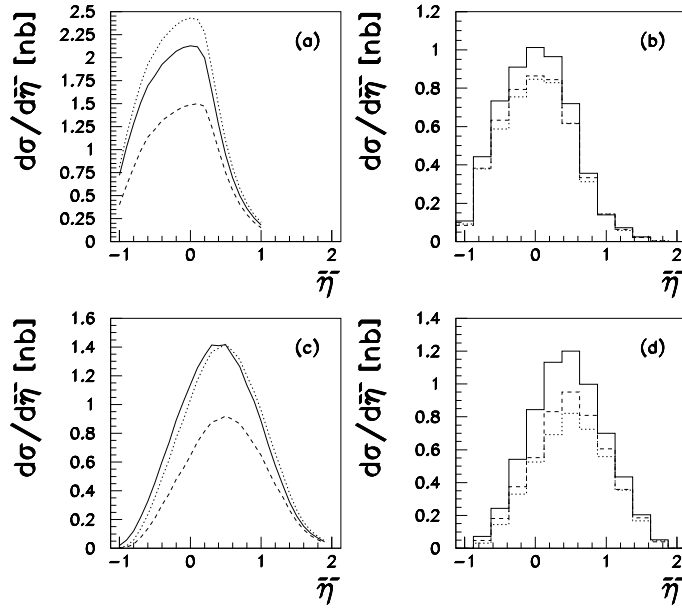


Figure 2: *NLO (left) and HERWIG (right) predictions for direct (top) and resolved (bottom) dijet cross sections $d\sigma/d\bar{\eta}$. We compare jet double counting (dotted), no R_{sep} (full), and $R_{\text{sep}} = 1$ (dashed) curves with EUCELL (full), PUCELL (dashed), and k_T (dotted) histograms.*

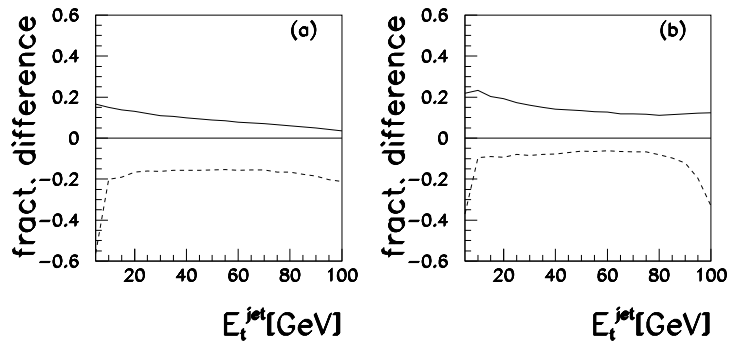


Figure 3: *E_T -dependence of the Snowmass jet definition uncertainties for a) direct and b) resolved dijet cross sections $d\sigma/dE_T$. We demonstrate the effects of jet double counting (full curves) and setting $R_{\text{sep}} = 1$ (dashed curves) compared to no double counting with $R_{\text{sep}} = 2$.*

(resolved) almost over the whole E_T -range. Only at the boundary of phase space at very large E_T , the fractional difference increases again. Thus, one should match the jet definitions at small and large E_T even more carefully.

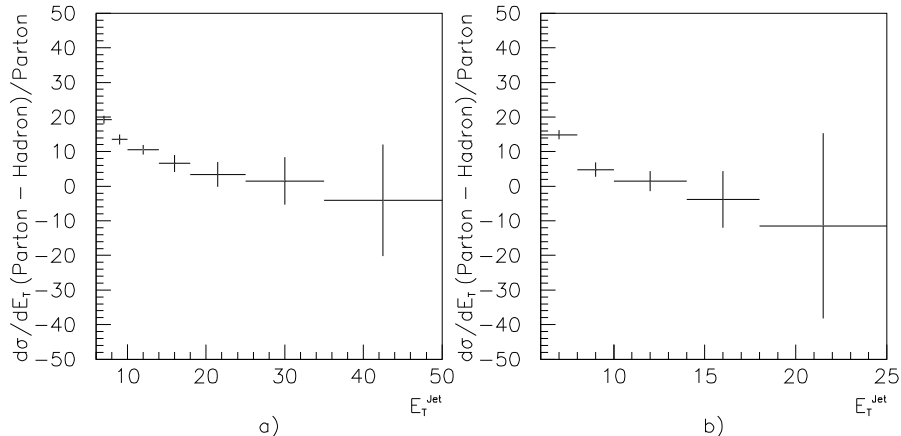


Figure 4: E_T -dependence of hadronization corrections for a) direct and b) resolved dijet cross sections $d\sigma/dE_T$.

The E_T -dependence of the hadronization corrections is shown in figure 4 for the a) direct and b) resolved dijet cross sections $d\sigma/dE_T$. We integrated again over the complete $\bar{\eta}$ range and over $\Delta\eta \in [-0.5, 0.5]$. At low transverse energies of $E_T \simeq 5$ GeV, the hadronization corrections amount to $\sim 20\%$ – a comparable effect to the theoretical uncertainties discussed before. They decrease very nicely towards larger E_T and vanish at 30 to 40 GeV to establish the correspondence between partonic and hadronic jets there. The error bars are due to limited statistics and could be drastically reduced with more computer time.

Finally, we estimate the benefit that can be obtained from an increased HERA luminosity of 250 pb^{-1} to constrain the photon and the proton parton densities. Figure 5 gives the number of jets produced as a function of x_γ^{OBS} (left), x_p^{OBS} (right), and transverse jet energy E_T , where the bin sizes reflect the approximate expected experimental resolution. The cuts applied to the dijet cross section are $y \in [0.2, 0.9]$, $E_T > 30$ GeV, and $\eta < 2$. If we require at least 100 events, where statistical and systematic errors start to be of comparable size, jets with transverse energies up to 55 GeV can be measured, where the jet double counting uncertainties and hadronization corrections are very much reduced. We can still test the photon structure at large E_T in the region of $x_\gamma^{\text{OBS}} = 0.4 - 1$ and the proton structure in the region $x_p^{\text{OBS}} = 0.05 - 0.3$.

4 Conclusions

Constraining the proton and photon structure functions in photoproduction of jets at HERA requires a good understanding of the jets in experiment and in theory. We used a new NLO calculation and simulated HERA data to match different experimental jet definitions (EUCCELL,

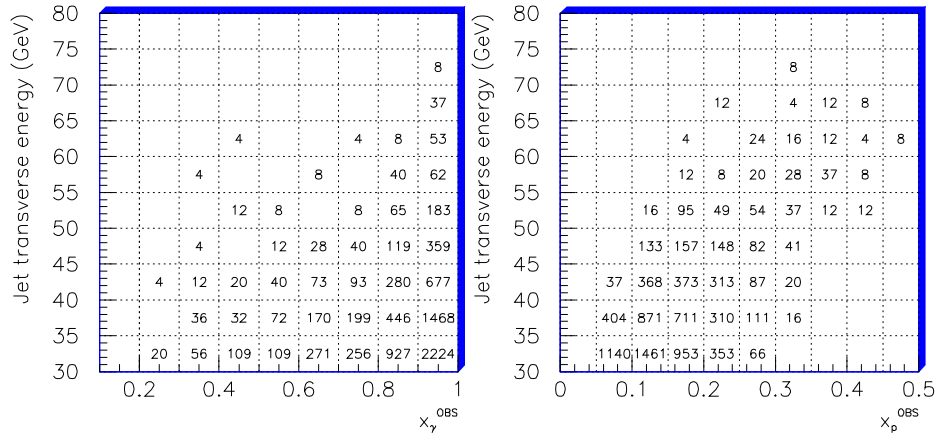


Figure 5: Number of events produced at an increased HERA luminosity of 250 pb^{-1} as a function of x_γ^{OBS} (left), x_p^{OBS} (right), and transverse jet energy E_T .

PUCCELL, and KTCLUS) with theory predictions with different values for the R_{sep} parameter. At larger transverse energies, the uncertainties from different theoretical jet definitions and hadronization corrections are reduced. These regions can be studied if the HERA luminosity is increased to 250 pb^{-1} , thus providing valuable information on the proton and photon structure functions over large x ranges.

References

- [1] M. Klasen, G. Kramer, to be published.
- [2] M. Klasen, G. Kramer, S.G. Salesch, Z. Phys. **C68** (1995) 113.
- [3] M. Derrick et al., ZEUS collaboration, Phys. Lett. **B348** (1995) 665.
- [4] S. Aid et al., H1 collaboration, Z. Phys. **C70** (1996) 17.
- [5] G. Marchesini et al., Comp. Phys. Comm. **67** (1992) 465.
- [6] J.E. Huth et al., Proc. of the 1990 DPF Summer Study on High Energy Physics, Snowmass, Colorado, edited by E.L. Berger, World Scientific, Singapore (1992) 134.
- [7] S. Catani, Yu.L. Dokshitzer, M.H. Seymour and B.R. Webber, Nucl. Phys. **B406** (1993) 187.
- [8] S.D. Ellis, D.E. Soper, Phys. Rev. **D48** (1993) 3160.
- [9] S.D. Ellis, Z. Kunszt, D.E. Soper, Phys. Rev. Lett. **69** (1992) 3615.